

Discovery of ^{109}Xe and ^{105}Te : Superaligned α Decay near Doubly Magic ^{100}Sn

S. N. Liddick,¹ R. Grzywacz,^{2,3} C. Mazzocchi,² R. D. Page,⁴ K. P. Rykaczewski,³ J. C. Batchelder,¹ C. R. Bingham,^{2,3} I. G. Darby,⁴ G. Drafta,² C. Goodin,⁵ C. J. Gross,³ J. H. Hamilton,⁵ A. A. Hecht,⁶ J. K. Hwang,⁵ S. Ilyushkin,⁷ D. T. Joss,⁴ A. Korgul,^{2,5,8,9} W. Królás,^{9,10} K. Lagergren,⁹ K. Li,⁵ M. N. Tantawy,² J. Thomson,⁴ and J. A. Winger^{1,7,9}

¹UNIRIB, Oak Ridge Associated Universities, Oak Ridge, Tennessee 37831, USA

²Department of Physics and Astronomy, University of Tennessee, Knoxville, Tennessee 37996, USA

³Physics Division, Oak Ridge National Laboratory, Oak Ridge, Tennessee 37831, USA

⁴Department of Physics, University of Liverpool, Liverpool L69 7ZE, United Kingdom

⁵Department of Physics and Astronomy, Vanderbilt University, Nashville, Tennessee 37235, USA

⁶Department of Chemistry, University of Maryland, College Park, Maryland 20742, USA

⁷Department of Physics and Astronomy, Mississippi State, Mississippi 39762, USA

⁸Institute of Experimental Physics, Warsaw University, Warszawa, PL 00-681, Poland

⁹Joint Institute for Heavy-Ion Research, Oak Ridge, Tennessee 37831, USA

¹⁰Institute of Nuclear Physics, Polish Academy of Sciences, PL 31-342 Kraków, Poland

(Received 16 May 2006; revised manuscript received 23 June 2006; published 21 August 2006)

Two new α emitters ^{109}Xe and ^{105}Te were identified through the observation of the $^{109}\text{Xe} \rightarrow ^{105}\text{Te} \rightarrow ^{101}\text{Sn}$ α -decay chain. The ^{109}Xe nuclei were produced in the fusion-evaporation reaction $^{54}\text{Fe}(^{58}\text{Ni}, 3n)^{109}\text{Xe}$ and studied using the Recoil Mass Spectrometer at the Holifield Radioactive Ion Beam Facility. Two transitions at $E_\alpha = 4062 \pm 7$ keV and $E_\alpha = 3918 \pm 9$ keV were interpreted as the $l = 2$ and $l = 0$ transitions from the $7/2^+$ ground state in ^{109}Xe ($T_{1/2} = 13 \pm 2$ ms) to the $5/2^+$ ground state and a $7/2^+$ excited state, located at 150 ± 13 keV in ^{105}Te . The observation of the subsequent decay of ^{105}Te marks the discovery of the lightest known α -decaying nucleus. The measured transition energy $E_\alpha = 4703 \pm 5$ keV and half-life $T_{1/2} = 620 \pm 70$ ns were used to determine the reduced α -decay width δ^2 . The ratio $\delta_{^{105}\text{Te}}^2 / \delta_{^{213}\text{Po}}^2$ of ~ 3 indicates a superallowed character of the α emission from ^{105}Te .

DOI: 10.1103/PhysRevLett.97.082501

PACS numbers: 23.60.+e, 21.10.Dr, 21.10.Pc, 27.60.+j

Alpha decay has long proven to be a useful tool to investigate the low-energy structure of neutron-deficient nuclides near magic shell closures [1]. The presence of an island of α emission in the neutron-deficient Sn region provided initial evidence that the $N, Z = 50$ shell closures apply to ^{100}Sn (e.g., [2,3]). In the classical Gamow picture, α decay occurs through the preformation of an α particle in the nucleus and its subsequent tunneling through Coulomb and centrifugal barriers [4]. Close to the $N = Z$ line, above ^{100}Sn , protons and neutrons are expected to occupy identical orbitals. This may result in an enhancement of the preformation probability of an α particle within the nucleus and the development of so-called superallowed α decay [2].

The low-energy structure of nuclei around doubly magic ^{100}Sn provides a benchmark for the development and interpretation of shell structure models. Significant recent work has been devoted to elucidate the single-particle structure around ^{100}Sn (e.g., Refs. [5–8]). While a shell-model description of the odd-mass Sn, Te, and Xe isotopes requires knowledge of five single-particle energies ($\nu d_{5/2}$, $\nu g_{7/2}$, $\nu s_{1/2}$, $\nu d_{3/2}$, $\nu h_{11/2}$), the energy separation between the lowest single-particle states $\nu d_{5/2}$ and $\nu g_{7/2}$ is of particular importance for the low-energy structure in these nuclei and yet they have not been measured. There are numerous theoretical estimates for the $\nu g_{7/2}$ - $\nu d_{5/2}$ energy separation which range from -0.05 to 1.9 MeV ([9,10],

and references therein). Experiments performed in this region investigating the low-energy structure of the Sn, Te, and Xe isotopes suggest that the $\nu g_{7/2}$ - $\nu d_{5/2}$ energy separation is below 0.3 MeV [5–9,11–14]. Experimental efforts are needed to improve this constraint and ultimately identify the low-energy excited states in ^{101}Sn . Further interest in the decay rates of nuclei around ^{100}Sn comes from the study of astrophysical processes, for which this region has been cited as the end of the rapid proton capture process due to the Sn-Sb-Te cycle [15].

The development of new experimental techniques has continually increased the number of nuclei that are accessible for spectroscopic study [5,6,16]. However, despite many experimental efforts [17,18], new neutron-deficient isotopes of Xe and Te have not been observed since the discovery of ^{110}Xe and ^{106}Te over 25 years ago [19]. The current work focuses on the first identification of ^{109}Xe and ^{105}Te through the observation of their α -decay chain. This marks the closest approach to the $N = Z$ line above ^{100}Sn and provides an opportunity to search for superallowed α decay and extends the $5/2^+$ and $7/2^+$ level systematics to ^{105}Te .

The ^{109}Xe nuclei were produced in the $^{54}\text{Fe}(^{58}\text{Ni}, 3n)^{109}\text{Xe}$ fusion-evaporation reaction with beam energies between 220 and 225 MeV on a $470 \mu\text{g}/\text{cm}^2$ thick ^{54}Fe target. Mass 109 reaction products were separated according to the ratio between atomic mass

and ionic charge using the Holifield Radioactive Ion Beam Facility Recoil Mass Spectrometer [20]. The separated beam passed through the mylar foil of a high efficiency microchannel plate counter, a 0.15 mg/cm² thick Al degrader, and implanted with ~ 60 MeV into a 40 mm \times 40 mm \times 66 μ m double-sided silicon strip detector (DSSD) with 1-mm wide strips. The DSSD and all ancillary detectors were read out by digital electronics [21]. To ensure that the sequential ^{109}Xe and ^{105}Te α decays (time difference of only hundreds of nanoseconds) were correctly recorded, a novel acquisition mode was developed. If a preamplifier signal was beyond a preset threshold, ~ 9.2 MeV, it was considered to be an implanted ion and the energy and time of the event were recorded. This limit was chosen to exceed the expected sum of the ^{109}Xe and ^{105}Te α energies. If a signal was below this limit, 25 μ s of the pulse shape (trace) was recorded starting 1 μ s before the leading edge. Examples of traces for the $^{109}\text{Xe} \rightarrow ^{105}\text{Te} \rightarrow ^{101}\text{Sn}$ α -decay chain are shown in Fig. 1. The ability to identify two α particles closely spaced in time, milliseconds after the correlated ion implantation into the DSSD, demonstrates an advantage of digital electronics.

A total of 100 α - α decay events were attributed to the $^{109}\text{Xe} \rightarrow ^{105}\text{Te} \rightarrow ^{101}\text{Sn}$ decay chain. The maximum time allowed between an implant and correlated decay events in the same DSSD pixel was limited to 200 ms. The energy calibration was obtained from known ^{109}Te and ^{108}Te α lines. The ^{108}Te resulted from the proton decay of ^{109}I .

The α energy spectra for ^{109}Xe and ^{105}Te are shown in Figs. 2(a) and 2(b). The energies of the two α transitions from ^{109}Xe are 3918 ± 9 and 4062 ± 7 keV. After decay-recoil energy correction the Q_α for the two transitions are 4067 ± 10 and 4217 ± 8 keV, respectively, leading to an energy of 150 ± 13 keV for the excited state in ^{105}Te . The

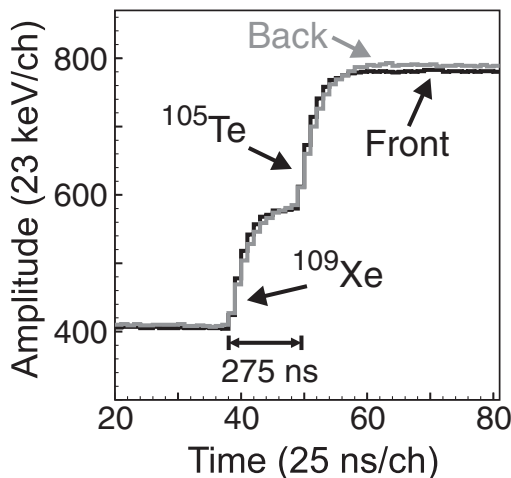


FIG. 1. Part of a signal trace, from 0.5 to 2.0 μ s, recorded for a $^{109}\text{Xe} \rightarrow ^{105}\text{Te} \rightarrow ^{101}\text{Sn}$ α -decay chain event. The time difference between the ^{109}Xe and ^{105}Te α particles is 275 ns, and traces from both the front (black line) and back (gray line) strips of the DSSD are shown.

α branching ratios to the excited and ground states of ^{105}Te are $(30 \pm 6)\%$ and $(70 \pm 6)\%$, respectively, assuming all ^{109}Xe decays proceed through α emission. The energy of the ^{105}Te α line is 4703 ± 5 keV, leading to Q_α of 4889 ± 6 keV. No fine structure was observed in the ^{105}Te α decay, but a 5% limit can be placed on the branching ratio of the decay to an excited state in ^{101}Sn .

The time distribution for the ^{109}Xe decay is shown on a logarithmic time axis in Fig. 2(c) constructed from the time difference between an implant in the DSSD and a subsequent correlated ^{109}Xe α decay. Using the method of Ref. [22] the half-life of ^{109}Xe is 13 ± 2 ms. The half-lives of the low and high energy α transitions from ^{109}Xe are 10 ± 3 ms and 15 ± 3 ms, respectively. The time distribution for ^{105}Te was derived by histogramming the time differences obtained from a fit to the ^{109}Xe - ^{105}Te double α traces. As the time between the two α pulses decreases, it becomes increasingly difficult for the analysis algorithm to identify the signal as a double pulse. The efficiency for identifying double pulses decreases at time differences below 0.5 μ s, though the algorithm is still sensitive to time differences as low as 0.25 μ s. The half-life of ^{105}Te is 620 ± 70 ns.

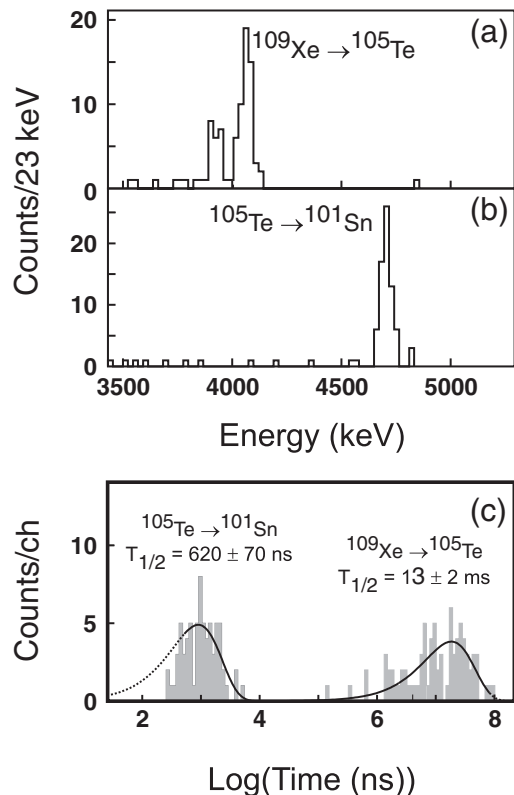


FIG. 2. Energy spectra from 3500 to 5250 keV for the α decay of (a) ^{109}Xe and (b) ^{105}Te . (c) Decay spectrum for ^{109}Xe and ^{105}Te on a logarithmic time axis and fit according to the method described in Ref. [22]. Only times above 0.5 μ s were used in the ^{105}Te half-life fit, which is indicated by the solid line.

The ground state spin and parity of ^{101}Sn was previously suggested to be $5/2^+$, arising from the $\nu d_{5/2}$ orbital [11]. The observation of only one α transition between ^{105}Te and ^{101}Sn suggests that the ground state of ^{105}Te is $I^\pi = 5/2^+$. A large α branch from ^{109}Xe to the excited state in ^{105}Te is interpreted as a result of the $l = 0$ character of the α transition which compensates for the decreased α energy compared to the higher energy $l = 2$ transition to the ground state. Thus the ground state of ^{109}Xe and the excited state of ^{105}Te are both tentatively assigned as $I^\pi = 7/2^+$ states, resulting in the decay scheme presented in Fig. 3. The spin and parity deduced for the ground state of ^{109}Xe agree with those proposed for the ^{111}Xe ground state [7] where in both cases excited levels have not been identified. The current results for ^{109}Xe are also consistent with the observation of fine structure in the α decay of ^{111}Xe to the tentative $5/2^+$ ground and $7/2^+$ first excited state in ^{107}Te [12]. The ordering of the ground and excited state in ^{105}Te agree systematically with those in the heavier $^{107,109,111}\text{Te}$ isotopes [7,13]. The $5/2^+$ and $7/2^+$ states in $^{109,111}\text{Te}$ have been identified as predominately having $\nu d_{5/2}$ and $\nu g_{7/2}$ parentage [13,14].

The Q_α values as a function of proton number are shown in Fig. 4(a) for nuclei in the ^{100}Sn and ^{208}Pb regions [23]. The expected increase in Q_α approaching doubly magic ^{100}Sn is observed in the new data for ^{109}Xe and ^{105}Te . In Fig. 4(b) the Q_α values for the Te and Xe isotopes are shown. When the odd- and even-mass isotopes are considered separately, there is an apparent linear trend between the neutron number and the Q_α value. If this systematic trend of the Q_α values is extended, Q_α for ^{104}Te can be expected to be greater than 5 MeV.

The reduced α -decay width δ^2 can be calculated using the tunneling probability P of an α particle through the potential barrier, using the WKB approximation, and the partial α -decay rate λ_α for a given transition, $\delta^2 = \lambda_\alpha h/P$. The reduced α -decay widths relative to ^{212}Po ($W_\alpha = \delta^2/\delta_{212\text{Po}}^2$) [16] for all three observed α transitions are

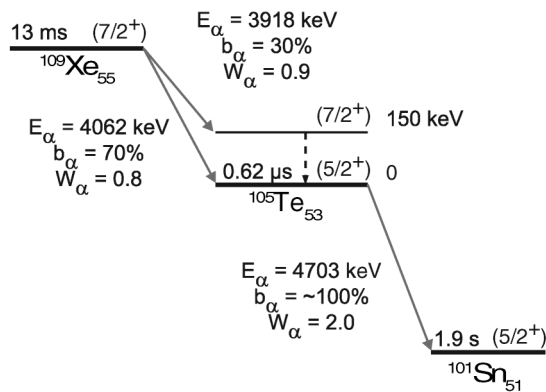


FIG. 3. Alpha decay scheme for the $^{109}\text{Xe} \rightarrow ^{105}\text{Te} \rightarrow ^{101}\text{Sn}$ decay chain. Figure is not to scale. See text for uncertainties on half-lives, energies, branching ratios, and W_α .

given in Fig. 3. The nucleus ^{212}Po is used as a reference for δ^2 values due to its simple nuclear structure; it may be pictured as an α cluster outside the doubly magic ^{208}Pb core [24]. The W_α values for the two ^{109}Xe transitions are 0.9 ± 0.3 to the ^{105}Te ground state and 0.8 ± 0.2 to the excited state. These widths should be considered upper limits since no consideration was given to other decay modes such as a small β branch (estimated as 4% assuming a $T_{1/2}^\beta$ of 368 ms [25]). The W_α of the ^{105}Te transition is 2.0 ± 0.3 . The difference between W_α for ^{109}Xe and ^{105}Te is not unexpected, as mixing between single-particle states becomes more pronounced away from the doubly magic ^{100}Sn .

When protons and neutrons occupy identical orbitals, the result may be an enhancement of the α preformation factor S , which is proportional to the α -decay width ($S = \delta^2/\nu h$, where ν is the frequency at which the α particle encounters the Coulomb barrier). A large increase in the preformation factor is expected to lead to superallowed α decay [3]. The W_α values for the lightest Te isotopes are compared to Po nuclei [23,26] with similar valence structure in Table I. An enhancement of 2.7 ± 0.7 is observed in the relative width of ^{105}Te compared to ^{213}Po , and it is apparent that the enhancement of α -decay widths is increasing as mass decreases suggesting that the $^{104}\text{Te} \rightarrow ^{100}\text{Sn}$ transition is the best candidate for superallowed α decay. Additionally, the enhancements for both ^{105}Te and ^{106}Te are consistent. However, since only two points are shown for odd and even masses it is difficult to determine how quickly the enhancement increases. Thus, a lower limit of the enhancement expected in ^{104}Te is taken to be 3. Combined with the extrapolated ^{104}Te Q_α an upper limit for the half-life of 100 ns for the α decay of ^{104}Te is

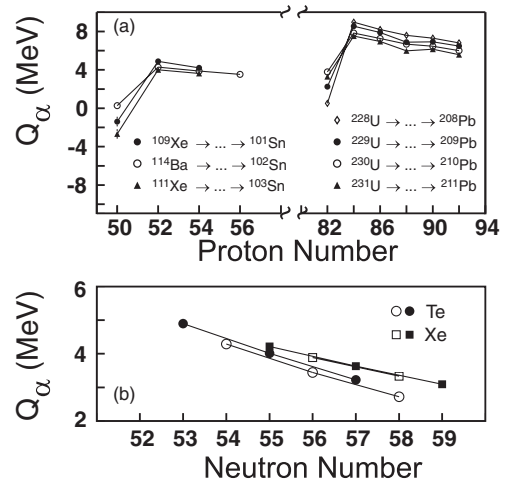


FIG. 4. (a) Q_α as a function of proton number for the different α decay chains in the ^{100}Sn and ^{208}Pb regions [23]. The strong double shell closures at ^{100}Sn and ^{208}Pb give rise to a peak in Q_α at proton numbers of 52 and 84, respectively. (b) Q_α for the ^{100}Sn region separated into even- and odd-mass α emitters.

TABLE I. W_α for isotopes in the $Z = 50$ and $Z = 82$ [23,26] regions. In each row are nuclei in the two different regions with corresponding valence structures with respect to the appropriate doubly magic core (either ^{100}Sn or ^{208}Pb). The last column shows the enhancement of the W_α value.

Valence	Nuclide	W_α	Nuclide	W_α	$W_\alpha^{\text{Te}}/W_\alpha^{\text{Po}}$
α	^{104}Te	3^a	^{212}Po	1.0	3^a
$\alpha + n$	^{105}Te	2.0 ± 0.3	^{213}Po	0.73 ± 0.14	2.7 ± 0.7
$\alpha + 2n$	^{106}Te	4.63 ± 0.56	^{214}Po	1.53 ± 0.02	3.02 ± 0.37
$\alpha + 3n$	^{107}Te	1.45 ± 0.63	^{215}Po	1.16 ± 0.01	1.25 ± 0.54
$\alpha + 4n$	^{108}Te	2.19 ± 0.27	^{216}Po	1.59 ± 0.01	1.38 ± 0.17

^aLower limit; see text for details.

deduced. The measurement of this half-life represents a significant experimental challenge but may still be feasible with the digital electronics used in our work.

An accurate understanding of nuclei around doubly magic ^{100}Sn requires a knowledge of single-particle energies, in particular, the energy separation between the $\nu d_{5/2}$ and $\nu g_{7/2}$ single-particle orbitals. Viewed from an extreme single-particle shell-model perspective, this energy separation can be extracted from the energy of the first excited state in ^{101}Sn . The energy systematics of $5/2^+$ and $7/2^+$ states as a function of neutron number can be extended to ^{105}Te (see Fig. 5). The simultaneous break with systematic trends at $N = 53$ for both Sn and Te isotopes may suggest that the $7/2^+$ level is converging toward the single-particle energy separation between the $\nu d_{5/2}$ and $\nu g_{7/2}$ single-particle orbits. Although configuration mixing may influence the trends, one could expect the excited $7/2^+$ state in ^{101}Sn to be around 160 keV.

In summary, the first identification of ^{109}Xe and ^{105}Te has been made through the detection of the α -decay chain

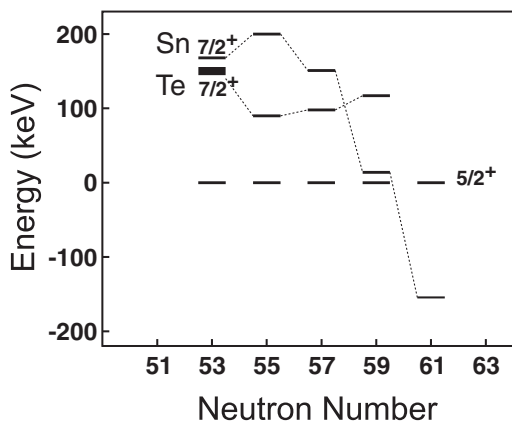


FIG. 5. Energy systematics of the $7/2^+$ level relative to the $5/2^+$ state for Te and Sn isotopes as a function of neutron number. Data were taken from the current work (heavy black line) and from Ref. [7] (and references therein).

$^{109}\text{Xe} \rightarrow ^{105}\text{Te} \rightarrow ^{101}\text{Sn}$ and marks the closest approach to the $N = Z$ line above ^{100}Sn . The half-lives of the two α decays were determined to be 13 ± 2 ms and 620 ± 70 ns for ^{109}Xe and ^{105}Te , respectively. The Q_α values are 4067 ± 10 and 4217 ± 8 keV for the α transitions from ^{109}Xe and 4889 ± 6 keV for the ^{105}Te α decay. The observed enhancement between the W_α for ^{105}Te and the analogous ^{213}Po indicates the superallowed character of the α decay of ^{105}Te . Fine structure was observed in the α decay of $^{109}\text{Xe} \rightarrow ^{105}\text{Te}$ placing the energy difference between the tentatively assigned $5/2^+$ ground state and $7/2^+$ excited state at 150 ± 13 keV. Further experiments are anticipated to measure both the fine structure in the ^{105}Te α decay to ^{101}Sn and attempt to measure the α -decay chain $^{108}\text{Xe} \rightarrow ^{104}\text{Te} \rightarrow ^{100}\text{Sn}$.

This work was supported in part by the UNIRIB consortium and under U.S. DOE Grants No. DE-AC05-06OR23100 (ORAU), No. DE-FG02-96ER40983 (UT), No. DE-AC05-00OR22725 (ORNL), No. DE-FG02-96ER-41006 (MississippiSU), and No. DE-FG05-88ER40407 (Vanderbilt), and the U.K. Engineering and Physical Sciences Research Council.

Note added in proof.— ^{105}Te has been independently identified by Seweryniak *et al.* [27].

- [1] A. Andreyev *et al.*, Nature (London) **405**, 430 (2000).
- [2] R.D. Macfarlane and A. Siivola, Phys. Rev. Lett. **14**, 114 (1965).
- [3] E. Roeckl, Radiochimica Acta **70/71**, 107 (1995).
- [4] G. Gamow, Z. Phys. **51**, 204 (1928).
- [5] C. Fahlander *et al.*, Phys. Rev. C **63**, 021307(R) (2001).
- [6] D. Seweryniak *et al.*, Phys. Rev. C **66**, 051307(R) (2002).
- [7] B. Hadinia *et al.*, Phys. Rev. C **70**, 064314 (2004).
- [8] H. Grawe *et al.*, Eur. Phys. J. A **27**, 257 (2006).
- [9] J. Ressler *et al.*, Phys. Rev. C **65**, 044330 (2002).
- [10] B.A. Brown *et al.*, Phys. Rev. C **50**, R2270 (1994).
- [11] O. Kavatsyuk *et al.*, GSI Report 2006-1 (to be published).
- [12] D. Schardt *et al.*, Nucl. Phys. **A326**, 65 (1979).
- [13] Zs. Dombrádi *et al.*, Phys. Rev. C **51**, 2394 (1995).
- [14] K. Starosta *et al.*, Phys. Rev. C **61**, 034308 (2000).
- [15] H. Schatz *et al.*, Phys. Rev. Lett. **86**, 3471 (2001).
- [16] Z. Janas *et al.*, Eur. Phys. J. A **23**, 197 (2005).
- [17] C. Mazzocchi *et al.*, Phys. Lett. B **532**, 29 (2002).
- [18] A. Hecht *et al.*, AIP Conf. Proc. **819**, 355 (2006).
- [19] D. Schardt *et al.*, Nucl. Phys. **A368**, 153 (1981).
- [20] C.J. Gross *et al.*, Nucl. Instrum. Methods Phys. Res., Sect. A **450**, 12 (2000).
- [21] R. Grzywacz, Nucl. Instrum. Methods Phys. Res., Sect. B **204**, 649 (2003).
- [22] K.-H. Schmidt *et al.*, Z. Phys. A **316**, 19 (1984).
- [23] G. Audi *et al.*, Nucl. Phys. **A729**, 337 (2003).
- [24] K. Varga *et al.*, Phys. Rev. Lett. **69**, 37 (1992).
- [25] P. Möller *et al.*, At. Data Nucl. Data Tables **66**, 131 (1997).
- [26] G. Audi *et al.*, Nucl. Phys. **A729**, 3 (2003).
- [27] D. Seweryniak *et al.*, Phys. Rev. C **73**, 061301(R) (2006).